Density Functional Theory Study of the Reaction Mechanism and Energetics of the Reduction of Hydrogen Peroxide by Ebselen, Ebselen Diselenide, and Ebselen Selenol

Jason K. Pearson and Russell J. Boyd*

Department of Chemistry, Dalhousie University, Halifax, Nova Scotia, Canada B3H 4J3

Received: February 22, 2007

Density functional theory calculations at the B3LYP/6-311++G(3df,3pd)//B3LYP/6-31G(d,p) level have been performed to elucidate the mechanism and reaction energetics for the reduction of hydrogen peroxide by ebselen, ebselen diselenide, ebselen selenol, and their sulfur analogues. The effects of solvation have been included with the CPCM model, and in the case of the selenol anion reaction, diffuse functions were used on heavy atoms for the geometry optimizations and thermochemical calculations. The topology of the electron density in each system was investigated using the quantum theory of atoms in molecules, and a detailed interpretation of the electronic charge and population data as well as the atomic energies is presented. Reaction free energy barriers for the oxidation of ebselen, ebselen diselenide, and ebselen selenol are 36.8, 38.4, and 32.5 kcal/mol, respectively, in good qualitative agreement with experiment. It is demonstrated that the oxidized selenium atom is significantly destabilized in all cases and that the exothermicity of the reactions is attributed to the peroxide oxygen atoms via reduction. The lower barrier to oxidation exhibited by the selenol is largely due to entropic effects in the reactant complex.

Introduction

Glutathione peroxidases (GPx) are a class of antioxidant enzymes containing selenium that protect against oxidative stress in the human body by catalyzing the reduction of harmful peroxides, particularly HOOH (Scheme 1).[1] The active site of GPx, and indeed all selenium-containing enzymes (selenoenzymes), contains what is commonly known as the 21st natural amino acid, selenocysteine (Sec). Sec is the selenol analogue of the thiol amino acid cysteine (Cys). Since oxidative stress has been implicated in a wide variety of degenerative human conditions including various disease states and even the process of aging,[2] much research has been devoted to understanding the roles of GPx.[3] Ebselen (**1**) (2-phenyl-1,2-benzisoselenazol-3(2*H*)-one) is a cyclic selenamide that has been extensively studied as an antioxidant and GPx mimic.[4] While many GPx mimics have been proposed, ebselen has attracted notable interest because of its anti-inflammatory, antiatherosclerotic, and cytoprotective properties in both in vitro and in vivo models.[5]

Although ebselen lacks a selenol moiety (Se−H) and therefore also lacks structural similarity to the active site Sec residue in any selenoenzyme, the selenamide bond is readily cleaved by thiol (Scheme 2) to afford a selenosulfide, which can then be converted to the selenol derivative of ebselen (**8**) by an additional thiol. In fact, a diselenide (**6**) can also be formed via the combination of the original ebselen molecule and the selenol derivative.[6] Scheme 2 illustrates the available pathways for interconversion of ebselen (**1**) to its diselenide (**6**) and selenol (**8**) derivatives and for the reduction of peroxides by each.

It is generally believed that the selenol form of ebselen (or the selenolate anion to be more precise) is the active form in terms of the reduction of hydrogen peroxide;[6,7−9] however, it is not without some degree of debate.[6,10] Indeed it would seem that the existence of a selenol functionality would be required for a GPx-like mechanism (i.e., **8** → **4** → **5**). Nevertheless, GPx

SCHEME 1: Catalytic Cycle of GPx

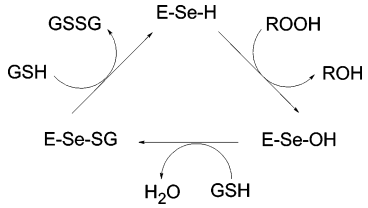

mimics in the literature have a wide range of structures[11,12] including selenamides,[11−18] diselenides,[13,19−26] allyl selenides,[13] aryl selenides,[27] and seleninate esters.[28] Although there are key differences, most of these compounds can be related to one of the three derivatives of ebselen in the redox map in Scheme 2. Consequently, each reductive pathway becomes an important piece of the puzzle in understanding selenium bioactivity, not just that of the selenol.

To date, there have been relatively few theoretical studies of organoselenium compounds and selenoenzymes. Molecular mechanics methods have been used to model the full catalytic cycle of GPx,[29] and the redox chemistry of small molecule GPx mimics has been investigated with ab initio and DFT methods using effective core potentials on selenium.[30] Also, the reaction between methyl thiolate and methyl selenolate with hydrogen peroxide has been studied using Møller−Plesset perturbation theory.[31] More recently, ebselen and ebselen selenol have been investigated by Mugesh to uncover the effects of intramolecular interactions on GPx activity.[32]

In a previous paper,[33] we reported reaction energetics (as well as structural and mechanistic information) for the reduction of hydrogen peroxide by a series of small organoselenium compounds representing ebselen, ebselen diselenide, and ebselen selenol. In that study a number of interesting conclusions were drawn: (i) The diselenide model was predicted to have the lowest activation energy (29.6 kcal/mol) by a significant margin over the selenol (49.4 kcal/mol) and the model ebselen

* E-mail: russell.boyd@dal.ca.

10.1021/jp071499n CCC: $37.00
Published on Web 04/04/2007

SCHEME 2: Summary of Proposed Catalytic Schemes Involving Reduction of Peroxides by Ebselen (1), Ebselen Diselenide (6), and Ebselen Selenol (8)

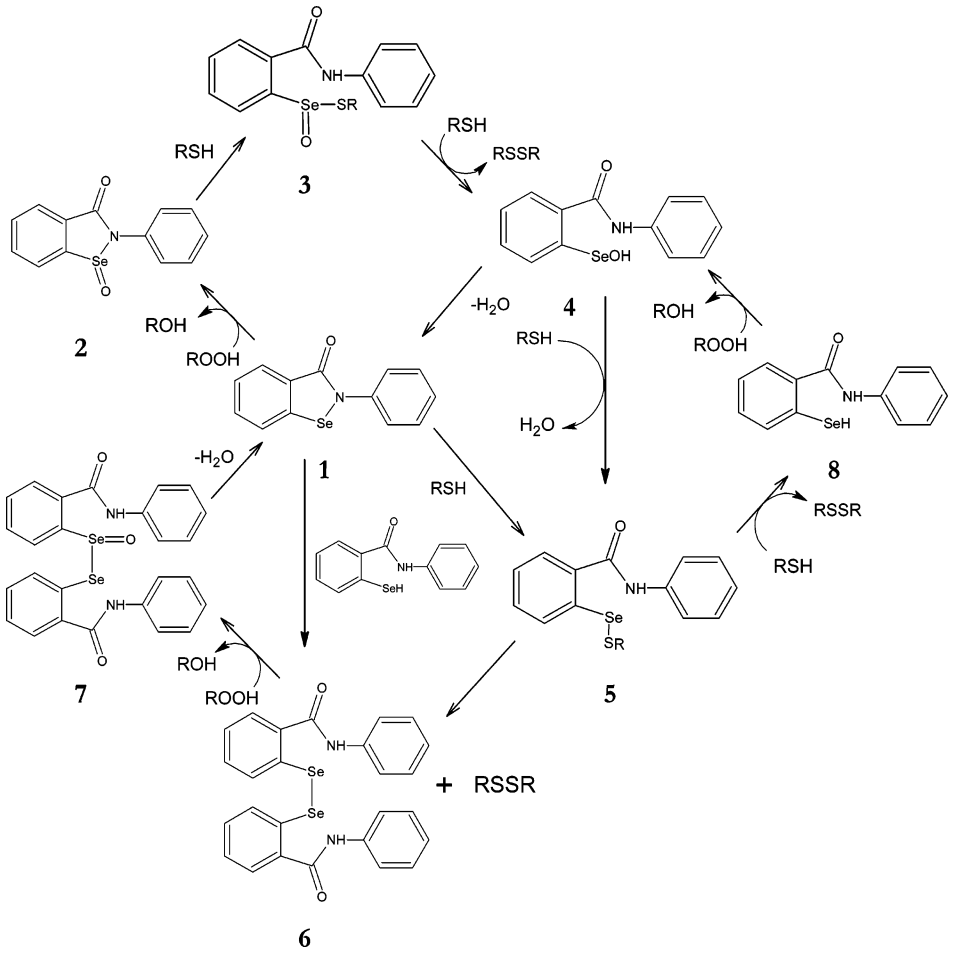

compound (60.2 kcal/mol). (ii) Upon oxidation of a diselenide, a selenoxide (Se═O) product should be formed rather than the experimentally suggested selenenic anhydride (Se−O−Se) (see Scheme 2).[11] (iii) The ebselen model was predicted to reduce hydrogen peroxide via a two-step hydrogen transfer mechanism, contrary to what experimental kinetics would indicate.

While it is now clear that the simple models of the ebselen system were insufficient to carry any significant predictive weight for the full molecules, the results still provide meaningful information regarding selenium antioxidant chemistry and should show some interesting parallels with the full molecules. The present study aims to gain greater insight by modeling the reduction of hydrogen peroxide by the full ebselen, ebselen diselenide, and ebselen selenol molecules. Additionally, this will afford us the opportunity to learn more about how the peroxide O−O bond is cleaved in oxidative processes involving HOOH. Peroxide oxygen transfer has been the focus of much research and debate.[34]

In accord with our previous paper,[33] a parallel study involving the sulfur analogues of the ebselen compounds is included. Because it is well-known that sulfur compounds are weaker reducing agents than their selenium-containing counterparts, they should have higher reaction barriers.

Computational Methods

All calculations were carried out with the AIM2000,[35] AIMPAC,[36] or the Gaussian 03[37] software packages. Geometry optimizations were performed with Becke's three-parameter exchange functional[38] (B3) in conjunction with the correlation functional proposed by Lee, Yang, and Parr (LYP) using the 6-31G(d,p) Pople basis set as suggested recently for the reliable prediction of organoselenium geometries and energetics.[39] Transition states were located using Schlegel's synchronous transit-guided quasi-Newton (STQN) method[40,41] and were linked to reactant and product complex structures by the use of intrinsic reaction coordinate calculations.[42,43] Frequency calculations were performed on all optimized structures using the B3LYP/6-31G(d,p) method to confirm whether a structure is a minimum or first-order saddle point, etc. A scaling factor of 0.9614[44] was used to obtain accurate thermochemical data. Accurate energies were obtained for all structures via single-point calculations using the 6-311++(3df,3pd) Pople basis set with the B3LYP method. It has been shown previously that bond dissociation energies (about the selenium atom) converge for similar systems without the use of effective core potentials using a 6-311G(2df,p) basis set;[39] however, the larger 6-311++G-(3df,3pd) basis was chosen based on the fact that it requires only a relatively modest increase in computational resources. Solvent effects for an aqueous environment (i.e., a dielectric constant of 78.39) were incorporated implicitly with single-point calculations using the conductor-like polarizable continuum model (CPCM) at the B3LYP/6-311++G(3df,3pd) level. Also, for the case of the selenol anion reaction, diffuse functions were included on heavy atoms for the geometry optimizations and frequency calculations as well as in the transition state searches.

The topology of the electron density was examined with the AIM2000[35] and AIMPAC[36] software packages using the gas-phase optimized wavefunctions.

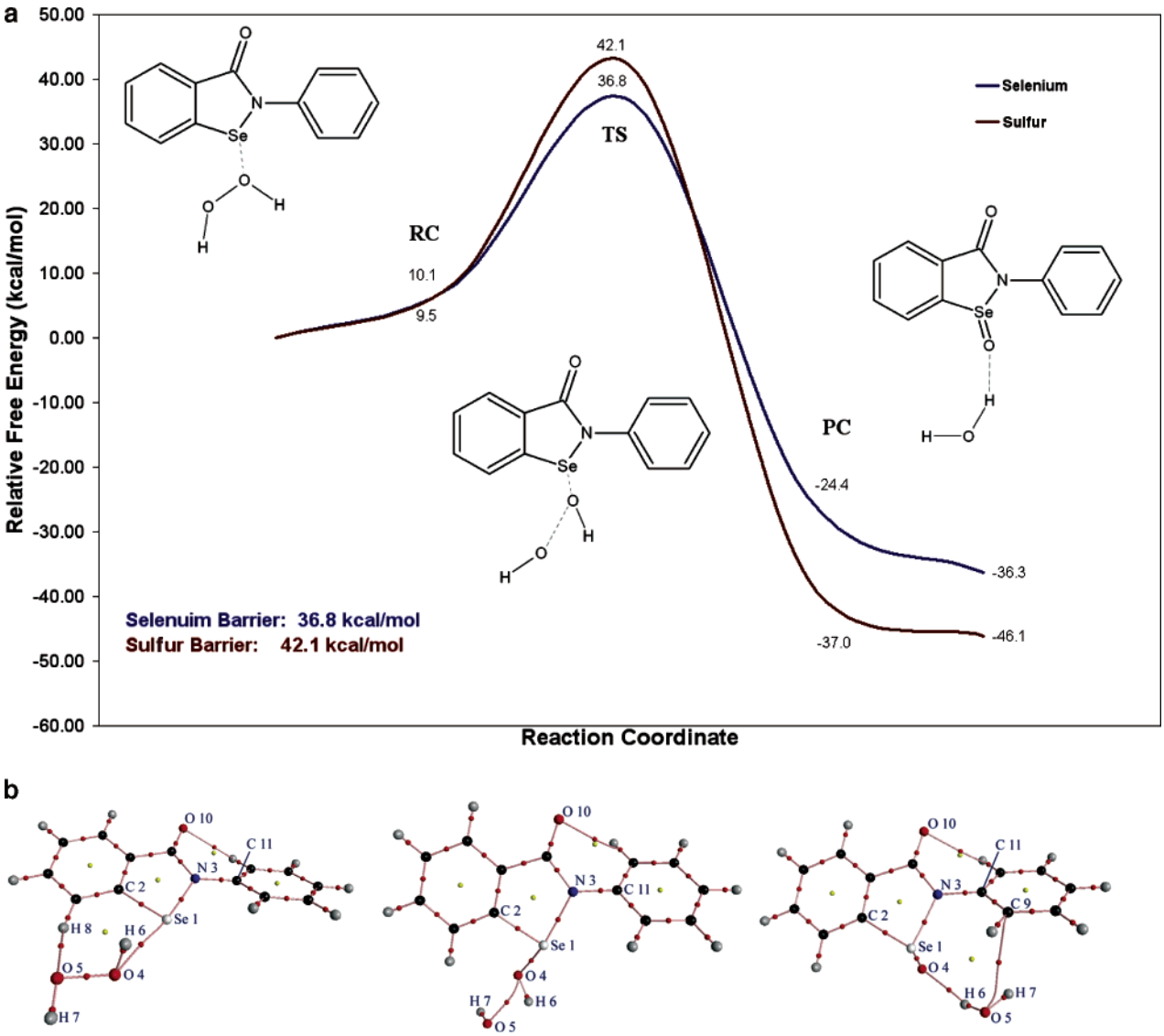

Figure 1. (a) Free energy profile of the ebselen reaction with hydrogen peroxide (**1** → **2**). Results are also presented for the sulfur analogue. (b) Molecular graphs of the reactant complex, transition state, and product complex showing positions of all nuclei, bond critical points (red dots), and ring critical points (yellow dots).

Results and Discussion

Figures 1−3 show the relative free energy profile along the reaction coordinate (obtained at the B3LYP/6-311++G-(3df,3pd) level including the CPCM solvation model at the B3LYP/6-31G(d,p) gas-phase geometry)[45] corresponding to oxidation of the three selenium compounds by hydrogen peroxide (shown in blue). The free energy profile for the sulfur analogue of each molecule is shown in red. The barriers in each case are calculated as the difference in free energy between the transition state complex (TS) and the infinitely separated reactant molecules.

Figures 1−3 also show the associated molecular graphs generated using the quantum theory of atoms in molecules (QTAIM).[46,47] These graphs illustrate the positions of maxima in electron density (nuclei) and the paths of maximum electron density that join bonded nuclei (bond paths). Also included in the molecular graphs are the positions of the bond critical points (BCPs), ring critical points (RCPs), and cage critical points (CCPs). The electron density at the BCP (ρ_{BCP}) has been proven to be a useful tool in characterizing the bonding between two atoms and is thus used as a measure of bond strength.[46,48] Furthermore, QTAIM results have been shown to be relatively insensitive to the choice of basis set and computational method. Generally, ρ_{BCP} values of >0.20 au are expected for covalent or polar covalent interactions while closed-shell interactions (such as H-bonding and ionic bonding) typically show a ρ_{BCP} of <0.10 au. Tables 1−3 include geometrical data from the gas-phase optimizations of all species at the B3LYP/6-31G(d,p) level as well as ρ_{BCP} values obtained using the B3LYP/6-31G(d,p) wavefunction.[45]

A QTAIM analysis also provides a decomposition of the overall energetics of each reaction into atomic contributions. This is accomplished by partitioning the electron density of a molecule into regions or basins defined by the zero-flux condition

$$\nabla\rho(\mathbf{r})\cdot\mathbf{n}(\mathbf{r}) = 0 \qquad \text{for all } \mathbf{r} \text{ on the surface} \qquad (1)$$

where $\nabla\rho(\mathbf{r})$ is the gradient of the electron density and $\mathbf{n}(\mathbf{r})$ is a unit vector normal to the surface. The basins correspond to the atoms in a molecule, and integration of the total electronic

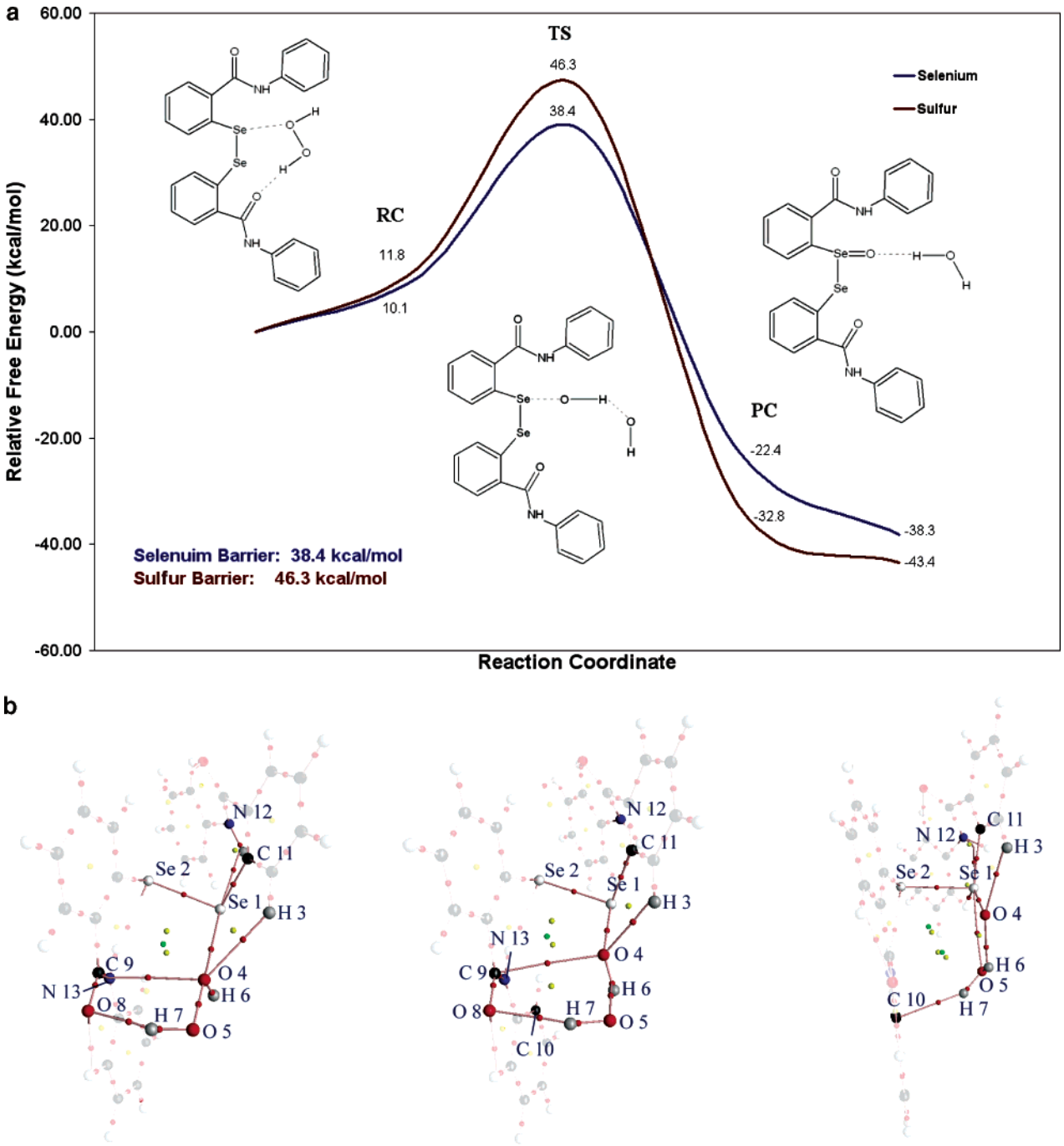

Figure 2. (a) Free energy profile of the ebselen diselenide reaction with hydrogen peroxide (**6** → **7**). Results are also presented for the sulfur analogue. (b) Molecular graphs of the reactant complex, transition state, and product complex showing positions of all nuclei, bond critical points (red dots), ring critical points (yellow dots), and cage critical points (green dots). Atoms not directly involved in the reaction have been faded for clarity.

energy density over such regions in space (Ω) yield the electronic energies of the particular atom of interest.

$$\int_{\Omega} E_e(\mathbf{r})\, d\mathbf{r} = E_e(\Omega) \tag{2}$$

Similarly, integration of the electron density over an atomic basin will yield the population of the basin ($N(\Omega)$).

$$N(\Omega) = \int_{\Omega} \rho(\mathbf{r})\, d\mathbf{r} \tag{3}$$

The atomic charge (q) is the difference between the nuclear charge and the electronic population. A QTAIM analysis provides insight into the atomic details of any chemical process and is hereto applied to the reduction of hydrogen peroxide by ebselen, ebselen diselenide, and ebselen selenol. The atomic energy data is presented graphically in Figures 4−6.

Ebselen Oxidation (1 → 2). In our previous work[33] the model ebselen compound was predicted to undergo a two-step hydrogen transfer mechanism upon oxidation. The experimental kinetics suggested otherwise and the actual ebselen system lacks the required protons for such a mechanism, so the full molecule oxidation was expected to proceed via a single-step process. This was indeed found to be the case as illustrated in Figure 1. In the reactant complex, the peroxide oxygen (q_O = - 0.61e) coordinates to the selenium atom (q_{Se} = 0.58e) of the ebselen molecule. The peroxide O−O bond is practically cleaved in the

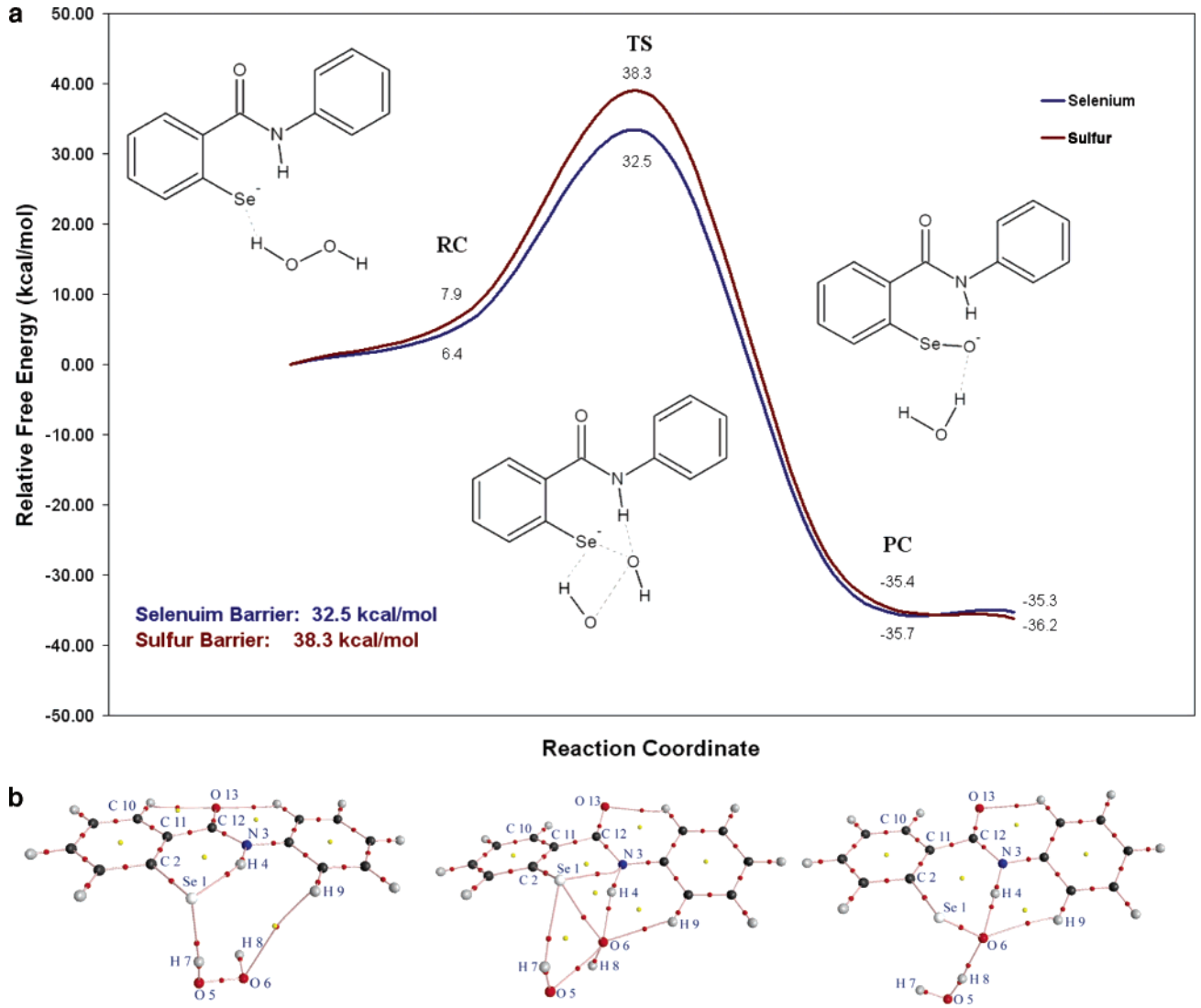

Figure 3. (a) Free energy profile of the ebselen selenol anion reaction with hydrogen peroxide (**8** → **4**). Results are also presented for the sulfur analogue. (b) Molecular graphs of the reactant complex, transition state, and product complex showing positions of all nuclei, bond critical points (red dots), and ring critical points (yellow dots).

TABLE 1: Interatomic Distances (*r*) and Bond Critical Point Electron Densities (ρ_{BCP}) of Relevant Interactions for the Reactant Complex (RC), Transition State (TS), and Product Complex (PC) of the Ebselen Oxidation Reaction

	RC		TS		PC	
	r (Å)	ρ_{BCP} (au)	*r* (Å)	ρ_{BCP} (au)	*r* (Å)	ρ_{BCP} (au)
Se_1-C_2	1.896	0.162	1.898	0.166	1.945	0.157
Se_1-N_3	1.901	0.141	1.965	0.126	1.930	0.138
Se_1-O_4	2.912	0.016	1.955	0.113	1.659	0.210
O_4-O_5	1.457	0.276	1.994	0.073		
O_4-H_6	0.972	0.363	0.992	0.326	1.968	0.027
O_5-H_6					0.975	0.351
O_5-H_7	0.971	0.366	0.971	0.361	0.966	0.363
O_5-H_8	2.476	0.009				
O_5-C_9					3.256	0.007

transition state (TS) as suggested by the dramatic decrease in ρ_{BCP} between the two atoms (see Table 1) however there is still a bond path connecting the two atoms. The reaction is facilitated by the peroxide "folding" in on itself to result in what can be interpreted as a simultaneous peroxide O−O cleavage and selenoxide bond formation. It is worth noting though, that in the TS there is no bond path between H6 and O5 suggesting that cleavage of the peroxide O−O bond occurs prior to the proton shift.

TABLE 2: Interatomic Distances (*r*) and Bond Critical Point Electron Densities (ρ_{BCP}) of Relevant Interactions for the Reactant Complex (RC), Transition State (TS), and Product Complex (PC) of the Ebselen Diselenide Oxidation Reaction

	RC		TS		PC	
	r (Å)	ρ_{BCP} (au)	*r* (Å)	ρ_{BCP} (au)	*r* (Å)	ρ_{BCP} (au)
Se_1-Se_2	2.347	0.102	2.357	0.102	2.430	0.092
Se_1-O_4	3.165	0.011	2.126	0.089	1.668	0.206
Se_1-O_5					2.901	0.016
H_3-O_4	2.349	0.013	2.169	0.020	2.315	0.016
O_4-O_5	1.454	0.278				
O_4-H_6	0.971	0.366	1.010	0.304	2.070	0.022
O_4-C_9	2.909	0.011	2.952	0.010		
O_5-H_7	0.983	0.351	0.975	0.356	0.968	0.361
O_5-H_6			1.481	0.095	0.973	0.354
H_7-O_8	1.860	0.030	2.117	0.017		
H_7-C_{10}					2.412	0.012

The free energy barrier of the ebselen oxidation reaction is predicted to be 36.8 kcal/mol. Previous experimental work by Morgenstern et al.[8] suggests that the activation energy for this reaction should be about 18.6 ± 0.2 kcal/mol. In contrast, the barrier for the oxidation of the sulfur analogue of ebselen is much greater (42.1 kcal/mol) owing to the experimentally

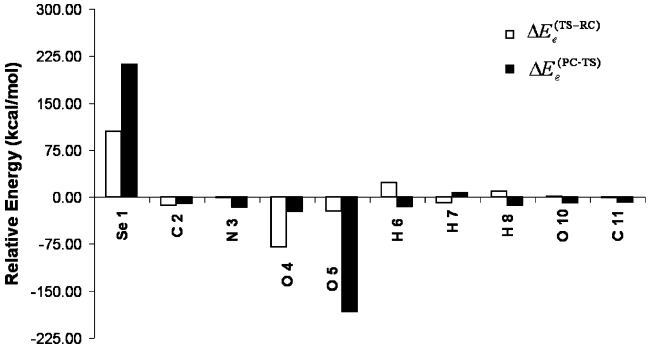

Figure 4. Atomic energy changes for the reaction of ebselen with hydrogen peroxide. The difference in atomic energy between the TS and RC, $\Delta E_e^{(TS-RC)}$, is presented as white bars while the difference in atomic energy between the PC and TS, $\Delta E_e^{(PC-TS)}$, is shown in black. A positive value indicates a destabilization while a negative value indicates a stabilizing effect. The atoms are labeled according to Figure 1b.

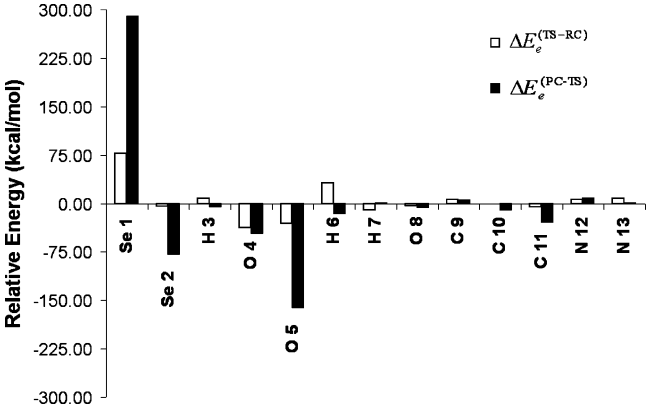

Figure 5. Atomic energy changes for the reaction of ebselen diselenide with hydrogen peroxide. The difference in atomic energy between the TS and RC, $\Delta E_e^{(TS-RC)}$ is presented as white bars while the difference in atomic energy between the PC and TS, $\Delta E_e^{(PC-TS)}$, is shown in black. A positive value indicates a destabilization while a negative value indicates a stabilizing effect. The atoms are labeled according to Figure 2b.

TABLE 3: Interatomic Distances (*r*) and Bond Critical Point Electron Densities (ρ_{BCP}) of Relevant Interactions for the Reactant Complex (RC), Transition State (TS), and Product Complex (PC) of the Ebselen Selenol Oxidation Reaction

	RC		TS		PC	
	r (Å)	ρ_{BCP} (au)	*r* (Å)	ρ_{BCP} (au)	*r* (Å)	ρ_{BCP} (au)
Se_1-C_2	1.916	0.149	1.893	0.158	1.937	0.150
Se_1-N_3			3.191	0.013		
Se_1-H_4	2.128	0.041				
Se_1-O_6			2.817	0.022	1.777	0.164
Se_1-H_7	2.289	0.029	2.473	0.017		
N_3-H_4	1.041	0.316	1.041	0.315	1.073	0.288
O_5-H_7	1.000	0.331	0.970	0.360	0.964	0.366
O_5-O_6	1.456	0.276	2.211	0.043		
O_5-H_8					1.000	0.322
O_6-H_4			1.701	0.045	1.535	0.073
O_6-H_8	0.971	0.367	0.968	0.356	1.703	0.046
O_6-H_9	3.667	0.001	2.272	0.015	2.457	0.011

confirmed decreased kinetic lability of the sulfur atom and thus shows good qualitative agreement with the experimental literature. Unfortunately, no experimental rate constants are known that correspond specifically to the sulfur analogues of these compounds of interest.

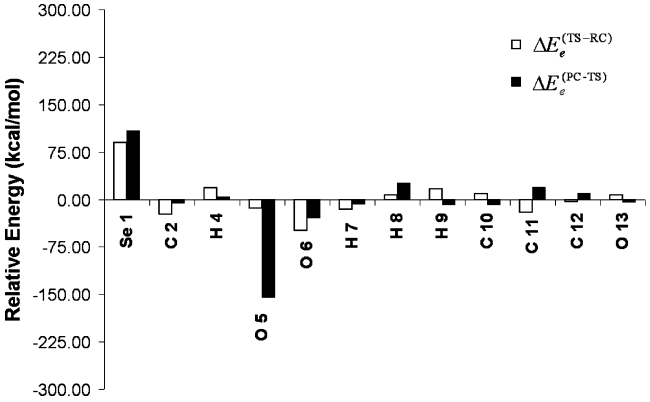

Figure 6. Atomic energy changes for the reaction of ebselen selenol with hydrogen peroxide. The difference in atomic energy between the TS and RC, $\Delta E_e^{(TS-RC)}$, is presented as white bars while the difference in atomic energy between the PC and TS, $\Delta E_e^{(PC-TS)}$, is shown in black. A positive value indicates a destabilization while a negative value indicates a stabilizing effect. The atoms are labeled according to Figure 3b.

Figure 4 illustrates the atomic electronic energy differences between the reactant complex (RC) and TS, $\Delta E_e^{(TS-RC)}$, and also between the TS and product complex (PC), $\Delta E_e^{(PC-TS)}$. A positive value indicates a destabilization and a negative value indicates that the atom has been stabilized. It is clear that the selenium atom and each of the peroxide oxygen atoms dominate the energy profile, as expected. The selenium atom is significantly destabilized along each step of the reaction coordinate, which is accompanied by a loss of electronic charge amounting to 0.36 e in the TS and an additional 0.58 e in the PC. This charge is almost entirely transferred to the peroxide oxygen atoms in each case. O5 is greatly stabilized by proceeding to the PC and thus the exothermic nature of the reaction is attributed to the increased stability of the water molecule relative to the original peroxide with a small contribution from the selenoxide oxygen (O4).

Ebselen Diselenide Oxidation (6 → 7). One of the most important findings in our model study[33] was that the oxidation of a model ebselen diselenide compound yields a selenoxide as opposed to the suggested selenenic anhydride. Such reactivity is not uncommon in organoselenium chemistry,[49] however all previous reports of ebselen diselenide oxidation have indicated that a selenenic anhydride is the expected product. This was an important motivator for pursuing the full molecule oxidation theoretically. While experimental investigation has led to the proposed selenenic anhydride product, the product of the diselenide oxidation is invariably a short-lived reactive intermediate that has not been observed. Kice and Chiou were the first to postulate the existence of the selenoxide but proposed it would exist only briefly before undergoing a fast isomerization to the selenenic anhydride.[50] Our calculations show, however, that the selenenic anhydride is actually higher in energy by ~7.7 kcal/mol and therefore may not be formed at all, at least not by a fast isomerization of **7**. As with the model diselenide, the predicted oxidation product of the full ebselen diselenide molecule is a selenoxide (**7**) as illustrated in Figure 2. Figure 2a shows that the predicted barrier to this reaction is approximately 38.4 kcal/mol as compared to the experimental value of 18.1 ± 0.1 kcal/mol.[8] Although the reaction barrier is overestimated by the computations, it is comparable to the calculated ebselen oxidation barrier and thus is in qualitative agreement with experiment. Considering that the oxidation of the ebselen diselenide theoretical model proceeds via a mech-

anism much like that of ebselen (see Figure 2b and Table 2) this is not surprising, and so interpretation of both theory and experiment in this complementary way supports the idea that the selenoxide is the preferred product. A key difference between ebselen and ebselen diselenide reactions is observed in terms of the peroxide O−O bond cleavage in the TS. The peroxide O−O bond is completely cleaved in the diselenide TS and a bond path exists between O5 and H6, contrary to the ebselen case. This shows that proton transfer has begun in the TS. It is also worth noting that the selenoxide bond is weaker for the diselenide TS than for the ebselen case.

The slightly higher barrier predicted for the diselenide can be explained by a comparison of the energy change of the peroxide oxygen atom (O4) in both systems (Figures 4 and 5). The main difference in these two diagrams is that in the ebselen case, O4 is stabilized to a greater extent in the TS than the diselenide. This is most likely due to the more complex bonding network in the diselenide case as illustrated by the molecular graph in Figure 2b, resulting in the electron density of the oxygen being shared by a greater number of atomic species. The peroxide oxygen in the diselenide case gains 0.17 e of electronic charge in the TS as compared to the ebselen system, where the peroxide oxygen atom gains 0.25 e of electronic charge, yielding a greater increase in stability.

Once again, the sulfur analogue produces a reaction barrier greater than that of the original diselenide (46.3 kcal/mol), further supporting the qualitative agreement between theory and experiment.

Ebselen Selenol Oxidation (8 → 4). While there have been arguments to support the diselenide as being the dominant form of ebselen in its glutathione peroxidase activity, more recent evidence strongly suggests that the selenol (**8**) (or selenolate anion to be more precise) is the most active redox form of ebselen in the redox map shown in Scheme 2.[11,12] In our model study,[33] the selenolate anion was not predicted to be the most active in reducing hydrogen peroxide but it was predicted to be more active than the neutral selenol and so it served as the focus for the full molecule investigation. The results for the full molecule study are presented in Figure 3 and Table 3. Figure 3a illustrates the calculated free energy profile for the ebselen selenolate anion (in blue) and its sulfur analogue (in red). The predicted barriers are 32.5 and 38.4 kcal/mol for the selenium and sulfur analogues, respectively. On the basis of the ebselen and ebselen diselenide free energy barriers in comparison with experimental activation energies (16.5 ± 0.1 kcal/mol for the ebselen selenol molecule),[8] the calculated barrier for the selenol case seems reasonable and thus the barriers of all systems qualitatively show good experimental agreement despite being overestimated. A stability analysis of the transition state wavefunctions for the selenolate and thiolate species in both the gas and solution phase shows internal instabilities with eigenvalues of the stability matrix ranging from −0.073 to −0.079. This is not uncommon for transition states corresponding to oxidation processes and has been reported previously.[30,31,51] Re-optimization of the wavefunctions produced energies 14 and 8 kcal/mol lower in the gas phase for the selenolate and thiolate systems, respectively; and 19 kcal/mol lower in the solution phase for both.

Comparison of the figures indicates that all three molecules are predicted to reduce hydrogen peroxide by a similar proton shift mechanism in which the peroxide "folds" in on itself donating a proton to the adjacent oxygen atom. Similar to the ebselen case, in the selenolate TS the peroxide O−O bond is not completely cleaved and no bond path yet exists between the peroxide oxygen (O5) and the shifting proton (H8). In contrast however, selenoxide bond formation is only weakly present in the TS as indicated by the ρ_{BCP} data in Table 3. In fact, the selenolate possesses the weakest TS selenoxide bond of all three compounds. The lower barrier associated with the selenol is largely due to entropic effects. Considering only the B3LYP/6-311++G(3df,3pd) CPCM electronic energy (i.e., neglecting the thermal correction to the Gibbs free energy), the selenolate RC lies in a well about 2.3 kcal/mol deep and the barrier to oxidation is almost exactly the same as that of ebselen; however, the ebselen RC does not lie in a potential well. The decrease in entropy upon forming a RC between the selenolate and peroxide leads to a destabilization of the RC in terms of the Gibbs free energy relative to the infinitely separated reactants, and thus the barrier is lowered by exactly the depth of the RC well, or roughly 2.3 kcal/mol. Also, despite the fact that the thermal correction to the Gibbs free energy yields a higher energy TS in all cases, the increase (relative to the separate reactants) is greater for both the ebselen and ebselen diselenide TS structures than the selenolate. The barriers for all reactions studied as well as other thermochemical data are summarized in Table 4.

TABLE 4: Summary of Gaseous Enthalpies, Entropies, and Free Energies of Activation for all Processes Studied in this Paper as Well as the Free Energy of Activation in Solution and the Overall Reaction Free Energy in Solution[a]

reaction	ΔH_a^{gas}	$T\Delta S_a^{gas}$	ΔG_a^{gas}	ΔG_a^{sol}	ΔG_{rxn}^{sol}
1 → **2**	22.8	−10.8	28.1	36.8	−36.3
1 → **2** (S analogue)	29.5	−11.1	37.2	42.1	−46.1
6 → **7**	30.8	−10.9	31.8	38.4	−38.3
6 → **7** (S analogue)	37.7	−13.3	42.2	46.3	−43.4
8 → **4**	25.1	−9.6	27.0	32.5	−35.7
8 → **4** (S analogue)	29.9	−9.9	32.0	38.3	−36.2

[a] All values in kcal/mol.

SCHEME 3: Interconversion between the Neutral Selenol (8) and Its Zwitterion (9)

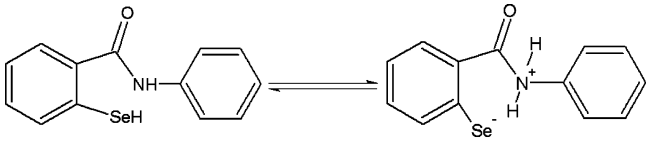

8 **9**

The calculated energetics of the selenolate oxidation by hydrogen peroxide are in good qualitative agreement with experiment. However, it was also prudent to probe the likelihood of the zwitterion (**9**) as a contributor to the reactivity of selenium-containing species. Therefore, the conversion of the neutral selenol to the zwitterion (Scheme 3) was investigated. Calculations on this system show that it is unlikely to be the most active reducing agent as it lies on an unstable potential energy surface. Table 5 lists the relative free energies for the conversion of the neutral selenol (**8**) to the zwitterion (**9**). The product (**9**) is nearly equal in energy to the transition state and thus is expected to be extremely short-lived if produced at all. Although the product is predicted to be higher in energy than the transition state for the B3LYP/6-311++G(3df,3pd) results, this is likely a result of the slight error introduced by calculating energies using a solvent model at a high-level basis set with the geometry of a lower level (i.e., B3LYP/6-31+G(d,p)). Sarma and Mugesh have also experimentally determined that the ebselen selenol zwitterion is an unstable isomer of **8**.[32] This

TABLE 5: Relative Free Energies (in kcal/mol) of the Neutral Selenol (8), the Selenol Zwitterion (9), and the Transition State That Connects Them Calculated at the B3LYP/6-31+G(d,p) Level and at the B3LYP/6311++G(3df,3pd)//B3LYP/6-31+G(d,p) Level Where, in the Latter Case, the Effects of Water Have Been Implicitly Included Using the CPCM Solvation Model

species	B3LYP/6-31+G(d,p)	B3LYP/6-311++G(3df,3pd)
8	0.0	0.0
TS **8** → **9**	15.7	16.9
9	15.7	17.0

evidence, combined with the fact that an aromatic selenol has a pK_a of approximately 6, suggests that the selenol anion is the most likely species to play a role in the GPx-like antioxidant behavior of ebselen selenol at physiological pH (i.e., ~7).

Analysis of the electronic population data for each case shows that the selenium atom losses 0.94−1.02 e of electronic charge by being oxidized, which is entirely transferred to the two peroxide oxygen atoms. In all cases, the oxygen atom of the resultant water molecule recovers the majority of electronic charge (~60%) while the selenoxide oxygen recovers the rest (~40%). The charge transfer for each case is slightly different in terms of when it takes place. For the ebselen and ebselen diselenide systems, the selenium atom loses 0.36 and 0.30 e of electronic charge at the TS, respectively, and loses an additional 0.58 and 0.72 e of electronic charge at the PC, respectively. The selenolate loses 0.47 e of electronic charge at both the TS and the PC, reflecting the lower barrier to oxidation.

Conclusions

A DFT study has been carried out on the reduction of hydrogen peroxide by ebselen (**1**), ebselen diselenide (**6**), and ebselen selenol (**8**). Calculations at the B3LYP/6-311++G-(3df,3pd) level with the CPCM implicit solvation model have been performed using B3LYP/6-31G(d,p) level gas-phase geometries to elucidate the mechanism and reaction energetics for these selenium-containing antioxidants. In the case of the selenol anion reaction, diffuse functions were used on heavy atoms for the geometry optimizations and thermochemical calculations.

Reaction free energy barriers for oxidation of the ebselen, ebselen diselenide, and ebselen selenol molecules are 36.8 kcal/mol, 38.4 kcal/mol, and 32.5 kcal/mol, respectively. These results are in good qualitative agreement with the available experimental literature. It has been found that the ebselen selenolate anion has the lowest barrier to oxidation by hydrogen peroxide. This has been attributed to entropic effects that both raise the energy of the RC and lower the energy of the TS relative to the ebselen and ebselen diselenide molecules. The oxidation in each case proceeds via a similar proton shift mechanism whereby the selenium atom loses roughly 1 e of electronic charge, which is largely recovered by the oxygen atoms of the resultant water molecule (~60%) and selenoxide (~40%). In all cases the selenium atom is significantly destabilized in the TS as well as the PC. The peroxide oxygen atoms, however, are stabilized in both the TS and PC and provide the driving force for the reaction. Analysis of the ρ_{BCP} data suggests that, for the ebselen and ebselen selenol reactions, proton shift occurs after the TS, while in the case of the diselenide, the peroxide O−O bond is completely cleaved and proton shift has begun.

The parallel study involving sulfur shows that, as expected, the sulfur analogues of these compounds are much poorer substrates and in general there is good qualitative agreement with experiment.

Acknowledgment. We gratefully acknowledge the Natural Sciences and Engineering Research Council of Canada (NSERC) and the Killam Trusts for financial support. We also acknowledge Leif Eriksson for thoughtful discussion as well as computational resources.

Supporting Information Available: Archive entries for geometry optimizations involved in Figures 1−3 (Tables S1, S2, and S3, respectively) and atomic integration data reported in Figures 4−6 (Tables S4, S5, and S6, respectively). This material is available free of charge via the Internet at http://pubs.acs.org.

References and Notes

(1) (a) Flohé, L.; Loschen, G.; Günzler, W. A.; Eichele, E. *Hoppe-Seyler's Z. Phsiol. Chem.* **1972**, *353*, 987. (b) *Selenium in Biology and Human Health*; Burk, R. F., Ed.; Springer-Verlag: New York, 1994. (c) Flohé, L. *Curr. Top. Cell Regul.* **1985**, *27*, 473. (d) Tappel, A. L. *Curr. Top. Cell Regul.* **1984**, *24*, 87. (e) Epp, O.; Ladenstein, R.; Wendel, A. *Eur. J. Biochem.* **1983**, *133*, 51. (f) Ganther, H. E. *Chem. Scr.* **1975**, *8a*, 79. (g) Ganther, H. E.; Kraus, R. J. In *Methods in Enzymology*; Colowick, S. P., Kaplan, N. O., Eds.; Academic Press: New York, 1984; Vol. 107, pp 593−602. (h) Stadtman, T. C. *J. Biol. Chem.* **1991**, *266*, 16257.

(2) (a) *Free Radicals in Biology*; Pryor, W. A., Ed.; Academic Press: New York, 1976−1982; Vols. 1−5. (b) *Free Radicals in Molecular Biology, Aging and Disease*; Armstrong, D., Sohal, R. S., Cutler, R. G., Slater, T. F., Eds.; Raven Press: New York, 1984.

(3) Flohé, L. In *Glutathione: Chemical, Biochemical and Medical Aspects*; Dolphin, D, Poulson, R., Avramovic, O., Eds.; John Wiley & Sons, Inc.: New York, NY, 1989; pp 643−731.

(4) (a) Müller, A.; Cadenas, E.; Graf, P.; Sies, H. *Biochem. Pharmacol.* **1984**, *33*, 3235. (b) Wendel, A.; Fausel, M.; Safayhi, H.; Tiegs, G.; Otter, R. *Biochem. Pharmacol.* **1984**, *33*, 3241. (c) Parnham, M. J.; Kindt, S. *Biochem. Pharmacol.* **1984**, *33*, 3247. (d) Müller, A.; Gabriel, H.; Sies, H. *Biochem. Pharmacol.* **1985**, *34*, 1185. (e) Safayhi, H.; Tiegs, G.; Wendel, A. *Biochem. Pharmacol.* **1985**, *34*, 2691. (f) Wendel, A.; Tiegs, G. *Biochem. Pharmacol.* **1986**, *35*, 2115.

(5) (a) Fong, M. C.; Schiesser, C. H. *Tetrahedron Lett.* **1995**, *36*, 7329. (b) Sies, H. *Free Radical Biol. Med.* **1993**, *14*, 313. (c) Sies, H. *Methods Enzymol.* **1994**, *234*, 476. (d) Schewe, T. *Gen. Pharmacol.* **1995**, *26*, 1153. (e) Nakamura, Y.; Feng, Q.; Kumagi, T.; Torikai, K.; Ohigashi, H.; Osawa, T.; Noguchi, N.; Niki, E.; Uchida, K. *J. Biol. Chem.* **2002**, *277*, 2687. (f) Zhang, M.; Nomura, A.; Uchida, Y.; Iijima, H.; Sakamoto, T.; Iishii, Y.; Morishima, Y.; Mochizuki, M.; Masuyama, K.; Hirano, K.; Sekizawa, K. *Free Radical Biol.* **2002**, *32*, 454.

(6) Zhao, R.; Holmgren, A. *J. Biol. Chem.* **2002**, *277*, 39456.

(7) Maiorino, M.; Roveri, A.; Coassin, M.; Ursini, F. *Biochem. Pharmacol.* **1988**, *37*, 2267.

(8) Morgenstern, R.; Cotgreave, I. A.; Engman, L. *Chem.-Biol. Interact.* **1992**, *84*, 77.

(9) Cotgreave, I. A.; Morgenstern, R.; Engman, L.; Ahokas, J. *Chem.-Biol. Interact.* **1992**, *84*, 69.

(10) Fischer, H.; Dereu, N. *Bull. Soc. Chim. Belg.* **1987**, *96*, 757.

(11) Mugesh, G.; Singh, H. *Chem. Soc. Rev.* **2000**, *29*, 347.

(12) Mugesh, G.; du Mont, W.; Sies, H. *Chem. Rev.* **2001**, *101*, 2125.

(13) Back, T. G.; Moussa, Z. *J. Am. Chem. Soc.* **2003**, *125*, 13455−13460.

(14) Mugesh, G.; Du Mont, W. W. *Chem. Eur. J.* **2001**, *7*, 1365.

(15) Reich, H. J.; Jasperse, C. P. *J. Am. Chem. Soc.* **1987**, *109*, 5549.

(16) Iwaoka, M.; Tomoda, S. *J. Am. Chem. Soc.* **1996**, *118*, 8077.

(17) Galet, V. et. al. *J. Med. Chem.* **1994**, *37*, 2903.

(18) Back, T. G.; Dyck, B. P. *J. Am. Chem. Soc.* **1997**, *119*, 2079.

(19) Mugesh, G.; Panda, A.; Singh, H. B.; Punekar, N. S.; Butcher, R. J. *J. Chem. Soc. Chem. Commun.* **1998**, 2227.

(20) Galet, V.; Bernier, J. L.; Heniehart, J. P.; Lesieur, D.; Abadie, C.; Rochette, L.; Lindenbaum, A.; Chalas, J.; Renaud de la Faverie, J. F.; Pfeiffer, B.; Renard, P. *J. Med. Chem.* **1994**, *37*, 2903.

(21) Iwaoka, M.; Tomoda, S. *J. Am. Chem. Soc.* **1994**, *116*, 2557.

(22) Wirth, T. *Molecules* **1998**, *3*, 164.

(23) Wilson, S. R.; Zucker, P. A.; Huang, R.-R. C.; Spector, A. *J. Am. Chem. Soc.* **1989**, *111*, 5936.

(24) Bailly, F.; Azaroual, N.; Bernier, J. L. *Bioorg. Med. Chem.* **2003**, *11*, 4623.

(25) Mugesh, G.; Panda, A.; Singh, H. B.; Punekar, N. S.; Butcher, R. J. *J. Am. Chem. Soc.* **2001**, *123*, 839.

(26) Nishibayashi, Y.; Singh, J. D.; Fukuzawa, S.; Uemura, S. *J. Org. Chem.* **1995**, *60*, 4114.

(27) Engman, L.; Stern, D.; Frisell, H.; Vessman, K.; Berglund, M.; Ek, B.; Andersson, C. *Bioorg. Med. Chem.* **1995**, *3*, 1255.

(28) Back, T. G.; Moussa, Z. *J. Am. Chem. Soc.* **2002**, *124*, 12104.

(29) Aumann, K. D.; Bedorf, N.; Brigelius-Flohé, R.; Schomburg, D.; Flohé, L. *BES* **1997**, *10*, 136.

(30) Benkova, Z.; Kóòa, J.; Gann, G.; Fabian, W. M. F. *Int. J. Quantum Chem.* **2002**, *90*, 555.

(31) Cardey, B.; Enescu, M. *Chem. Phys. Chem.* **2005**, *6*, 1175.

(32) Sarma, B. K.; Mugesh, G. *J. Am. Chem. Soc.* **2005**, *127*, 11477.

(33) Pearson, J. K.; Boyd, R. J. *J. Phys. Chem.* **2006**, *110*, 8979.

(34) (a) Curci, R. *Advances in Oxygenated Processes*; Baumstark, A. L., Ed.; JAI Press: Greenwich, CT, 1990; Vol. 2, Chapter 1, pp 1−59. (b) Curci, R.; Edwards, J.O. In *Catalytic Oxidations with H_2O_2 as Oxidants*; Strukul, G., Ed.; Series: Catalysis by Metal Complexes; Reidel-Kluwar: Dordrecht, The Netherlands, 1992; Chapter 3. (c) Sharpless, K. B.; Woodard, S. S.; Finn, M. G. *Pure Appl. Chem.* **1983**, *55*, 1823. (d) DiFuria, F.; Modean, G. *Pure Appl. Chem.* **1982**, *54*, 1853. (e) Swern, D. *Organic Peroxides*; Wiley-Interscience: New York, 1971; Vol. 2, pp 73−74

(35) Biegler-König, F. W.; Schönbohm, J.; Bayles, D. *J. Comput. Chem.* **2001**, *22*, 545.

(36) The AIMPAC suite of programs may be downloaded from Richard Bader's website: www.chemistry.mcmaster.ca/bader.

(37) *Gaussian 03, Revision B.05*; Frisch, M. J.; et al. Gaussian, Inc.: Pittsburgh, PA, 2003.

(38) Becke, A. D. *J. Chem. Phys.* **1993**, *98*, 5648.

(39) Pearson, J. K.; Ban, F.; Boyd, R. J. *J. Phys. Chem.* **2005**, *109*, 10373.

(40) Peng, C; Schlegel, H. B. *Isr. J. Chem.* **1993**, *33*, 449.

(41) Peng, C.; Ayala, P. Y.; Schlegel, H. B.; Frisch, M. J. *J. Comput. Chem.* **1996**, *17*, 49.

(42) Gonzalez, C.; Schlegel, H. B. *J. Chem. Phys.* **1989**, *90*, 2154.

(43) Gonzalez, C.; Schlegel, H. B. *J. Phys. Chem.* **1990**, *94*, 5523.

(44) Scott, A. P.; Radom, L. *J. Phys. Chem.* **1996**, *100*, 16502.

(45) Note that for the ebselen selenol anion, the B3LYP/6-31+G(d,p) method was used for geometry optimizations and frequency analyses to account for the diffuse electron density of the anionic selenium atom.

(46) Bader, R. F. W. *Atoms in Molecules: A Quantum Theory*; Oxford University Press: Oxford, U.K., 1990.

(47) *The Quantum Theory of Atoms in Molecules*; Matta, C.F., Boyd, R.J., Eds.; WILEY-VCH: Weinheim, 2007.

(48) (a) Bader, R. F. W. *J. Phys. Chem.* **1998**, *102*, 7314−7323. (b) Knop, O.; Boyd, R. J.; Choi, S. C. *J. Am. Chem. Soc.* **1988**, *110*, 7299.

(49) (a) Reich, H. J.; Hoeger, C. A.; Willis, W. W., Jr. *J. Am. Chem. Soc.* **1982**, *104*, 2936. (b) Block, E.; Birringer, M.; Chunhong, H. *Angew. Chem., Int. Ed.* **1999**, *38*, 1604. (c) Block, E.; et. al. *J. Am. Chem. Soc.* **2000**, *122*, 5052.

(50) Kice, J. L.; Chiou, S. *J. Org. Chem.* **1986**, *51*, 290.

(51) (a) Bach, R. D.; Winter, J. E.; McDouall, J. J. W. *J. Am. Chem. Soc.* **1995**, *117*, 8586. (b) Benassi, R.; Fiandri, L. G.; Taddei, F. *J. Org. Chem.* **1997**, *62*, 8018. (c) Bach, R. D.; Su, M. D.; Schlegel, H. B. *J. Am. Chem. Soc.* **1994**, *116*, 5379. (d) Baboul, A. G.; Schlegel, H. B.; Glukhovtsev, M. N.; Bach, R. D. *J. Comput. Chem.* **1998**, *19*, 1353. (e) Bach, R. D.; Andres, J. L.; Su, M. D.; McDouall, J. J. W. *J. Am. Chem. Soc.* **1993**, *115*, 5768.